

Formation of type-II excitons in CdTe/Cd_{1-x}Mn_xTe superlattices at high magnetic fields

H. H. Cheng

Center for Condensed Matter Sciences, Taiwan University, 1, Roosevelt Road, Section 4, Taipei, Taiwan

R. J. Nicholas

Department of Physics, Clarendon Laboratory, University of Oxford, Parks Road, Oxford, OX1 3PU, United Kingdom

D. E. Ashenford and B. Lunn

Department of Engineering Design and Manufacture, Hull University, Kingston-upon-Hull, HU6 7RX Humberside, United Kingdom

(Received 9 May 1997)

We report measurements of magnetorefectivity in CdTe/Cd_{1-x}Mn_xTe superlattices with varying manganese concentration in magnetic fields up to 45 T. From an analysis of the 1s heavy-hole σ_+ transition, we observe that the energy shift is directly equal to the shift in the valence-band edge of the barrier layer. This provides a clear proof of type-I–type-II crossover in this system. The critical magnetic field that leads to the formation of a type-II exciton is also estimated. We point out that the criterion for the observation of a type-II exciton is that the type-II valence-band offset has to be larger than the binding energy of an exciton. [S0163-1829(97)08640-2]

II-VI semimagnetic semiconductors have a large energy shift of the band edge due to the *sp-d* exchange interaction. In CdTe/Cd_{1-x}Mn_xTe quantum wells the confinement potential can therefore be continuously “tuned” by the exchange interaction. This has led several authors to search for evidence of a magnetic-field-induced transition from a type-I to a type-II band alignment. Based on the optical observation of a plateau in transition energy and a drop in the oscillator strength, a band alignment crossover has been reported in structures containing relatively low manganese contents.^{1,2} However, the results have proved to be controversial due to the complications introduced by the Coulomb interaction. This has led Kuroda *et al.*³ to extend the study to higher *x*-values and very high magnetic fields (≈ 150 T) where the magnetic interactions can dominate the Coulomb interaction and the transition energy is governed by the strong diamagnetic shift. A new feature above the 1s heavy-hole transition was reported. Nevertheless, it was not possible to determine whether or not a type-I–type-II crossover had occurred.

In this paper we present an interband magnetorefectivity measurement on a series of CdTe/Cd_{1-x}Mn_xTe superlattices with both low and high manganese concentrations at high magnetic fields up to 45 T. For low *x*, a strong asymmetric splitting between the σ_+ and σ_- components is observed at high fields, reflecting a different binding energy of the excitons. For the high *x* samples at high fields, the shift of the transition energy for σ_+ is equal to the valence-band edge tuning of the barrier layer, providing unambiguous experimental evidence of the type-I–type-II crossover in this system. From the analysis, the criterion for the observation of a type-II exciton is found to be when the type-II band offset is larger than the binding energy of an exciton.

A series of superlattice (SL) samples were grown by MBE on lattice-matched InSb substrates at Hull University. Long period samples are studied, which consist typically of a thick (1000 Å) CdTe buffer layer followed by 15 alternating layers of CdTe and Cd_{1-x}Mn_xTe with nominal well (bar-

rier) widths of 50 Å (150 Å) and varying manganese contents ranging from 2% to 11%. Magnetorefectivity was studied in the Faraday configuration (*B* perpendicular to the SL plane) using long pulsed (10 msec) magnetic fields up to 45 T, and a pulsed light source (Hg vapor lamp) fired at the peak field for a period of 500 μ sec. The samples were placed in the pulsed field center and immersed in liquid helium. The reflected light was collected using a fiber bundle and analyzed using a 0.25-m spectrometer and nitrogen-cooled charge-coupled-device detector.

The zero field reflectivity spectrum for a typical sample is shown in Fig. 1. The spectrum is ratioed against a metallic mirror response from the light source, using the same optical path, and shows a sharp minimum (or maximum) for the excitonic features around the region of both the barrier and SL band gap. The SL transition can give rise to both maxima and minima in the reflectivity, depending on the overall phase of the interference structure from the layers. The assignment of maxima or minima to the precise transition features was made using the full family of magnetorefectivity spectra (cf. Fig. 2) where the presence of peak sharpening generally made the specific assignment unambiguous. The feature at 1594.5 meV is due to the 1s exciton of the CdTe buffer layer and the higher energy transition corresponds to the band gap of the Cd_{1-x}Mn_xTe barriers. The observed SL excitonic transitions are the heavy hole to the ground state of the conduction band (*E*1) and light hole to *E*1, labeled as 1HH, 1LH, respectively. As the well width decreases, the energy of the 1HH and 1LH transitions moves upwards due to the increase of confinement energy. The potential height that determines the confinement energy depends on the band offset ratio and the strain due to the lattice mismatch of CdTe and Cd_{1-x}Mn_xTe. The strain, for the structures studied here, is accommodated in the magnetic layers as biaxial compression, whereas the quantum wells (nonmagnetic layers) are not strained due to the lattice match with the buffer layer. This lifts the degeneracy at the zone center for the barriers,

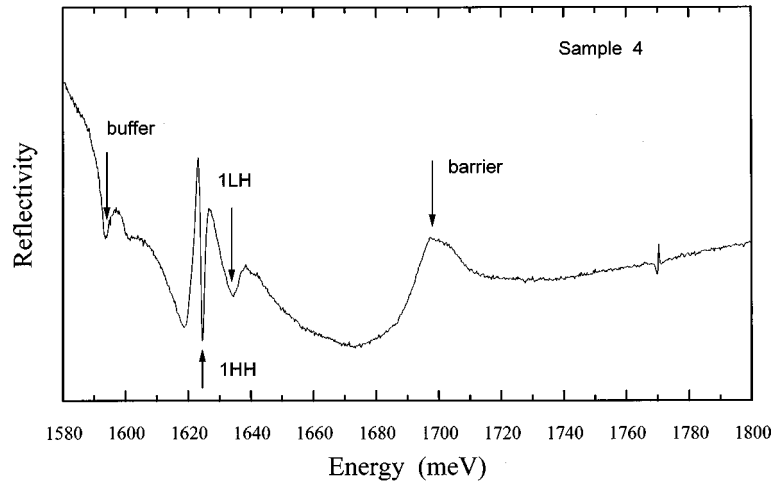


FIG. 1. Zero-field reflectivity spectrum of sample 4 showing the assignment of the transition of buffer, SL (1HH, 1LH) and barrier.

resulting in different potential heights for both conduction and valence band in the quantum well. A summary of the zero-field transition energies and fitted parameters is given in Table I.

The precise Mn concentration of the samples is determined from the barrier transition energy using $E = E_g + 1592 \times x - E_{\text{bulk}}$ where E_g is the CdTe band gap of 1606 meV and 1592 is the constant characterising the change of band gap with manganese concentration, E_{bulk} is the bulk (CdTe) exciton binding energy of 11.5 meV. Conduction-band (CB) and valence-band (VB) offset are deduced by using a band offset ratio $\Delta E_c/\Delta E_v$ of 70/30 following Kuhn-Heinrich *et al.*⁴ The well (barrier) width is the fitted value using the excitonic model of Ref. 5, E_b is the calculated exciton binding energy, and E_e and E_h are the confinement energies of the first subband of the electron and heavy hole.

Reflectivity spectra in pulsed magnetic fields for sample 4 are shown in Fig. 2. On applying magnetic fields, the 1s transition of the CdTe buffer moves upward in energy with increasing absorption strength. In some samples (number 2 and 5), it is sufficiently narrow to resolve a splitting at high

field due to spin. The oscillator strength of the transition increases with field, indicating a reduction of the cyclotron orbit (by 45 T it has increased by approximately a factor of 3). The barrier and SL transitions each split into two components corresponding to the σ_+ ($m_{hj} = -3/2$ to $m_{ej} = -1/2$) and σ_- ($m_{hj} = +3/2$ to $m_{ej} = +1/2$) transitions. In Fig. 2, we mark the movement of the excitonic transitions with field. The solid line indicates the CdTe buffer transition, the dashed line the 1HH transition, and the dotted line indicates the barrier transition. Other features can be seen but their movement with field is not indicated.

We first discuss the excitonic behavior of the barrier layer. The observed splitting is a consequence of the $sp-d$ exchange interaction and the diamagnetic energy. To obtain the exchange shift, the diamagnetic shift is subtracted from the observed σ_+ transition. The field-dependent energy shift is plotted in Fig. 3 (the diamagnetic shift has been assumed to be similar to that observed for the CdTe buffer layer due to the low manganese concentration). It shows an increase of the exchange splitting with increasing manganese concentration as discussed by Nicholas *et al.*⁶ and Isaacs *et al.*⁷ For

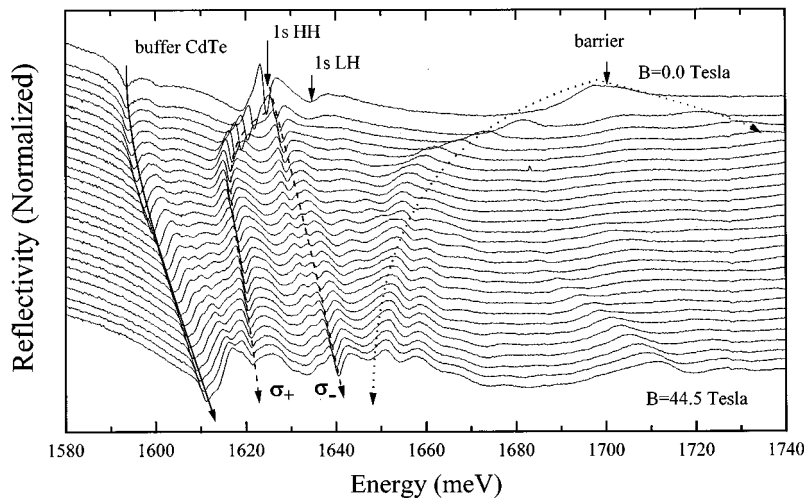


FIG. 2. A family of reflectivity spectra in pulsed fields from 0 to 44.5 T of sample 4. The solid (dashed) line indicates the 1s HH transition of buffer layer (SL). The dotted line is the barrier transition.

TABLE I. Summary of zero field transition energies and fitted well and barrier widths. CB and VB denote conduction and valence band, respectively.

Sample number	Mn (%)	CB (VB)		Barrier (meV)	Well (barrier)		E_e (E_h) (meV)	E_b (meV)	B_c (T)
		offset (meV)	HH1- E_1 (meV)		width (Å)				
1	0.6	6.4 (2.5)	1599.7	1604.4	80 (180)	5.2 (1.7)	12.0		
2	2.6	27.6 (10.9)	1608.2	1637.3	80 (180)	14.4 (3.9)	15.2	2	
3	5.0	53.0 (21.0)	1619.4	1674.4	66 (170)	24.6 (6.5)	16.9	3	
4	6.4	67.9 (27.0)	1624.2	1696.9	62 (170)	29.7 (7.7)	17.7	7	
5	7.3	77.4 (30.8)	1633.4	1710.8	52 (150)	36.3 (9.7)	18.2	8	
6	11	116.6 (46.4)	1660	1770	41 (140)	58.3(15)	19.6	15	

sample 6, the exchange splitting in the magnetic layers is not resolved, therefore the splitting taken from a bulk sample with a similar Mn^{2+} concentration of 10% which is plotted and will be used for the later discussion.

Next, we move to the SL transitions. The field-induced exchange splitting of the magnetic layer modifies the zero field potential height of the quantum wells, resulting in an ‘‘effective potential height’’ for the different spin states. As a consequence the SL transitions of the σ_+ and σ_- components also split in a similar way to the barrier layers due to the change of confinement energies. In this work, since we are interested in the type-I–type-II crossover, we therefore concentrate on the lowest transition of the σ_+ component. To see more clearly the excitonic splitting, the energy shift with respect to the zero field transition energy (ΔE_{HH}) is plotted in Fig. 4 for the five samples studied in detail as a function of magnetic fields, but without any correction for the diamagnetic shift of the excitons. At low field, this shows a rapid decrease in energy reflecting the decrease of the confinement energy of both the conduction and valence band. By 8 T it has fallen by approximately 8 and 12 meV for the lowest and highest concentration samples. Since the tuning of the VB is four times larger than the CB (Ref. 8) the drop in transition energy is mainly contributed by the VB. On increasing the magnetic field, the valence-band edge of $m_j = -3/2$ in the magnetic layers continues to rise. Hence a type-II band structure is expected where electrons are con-

finned in nonmagnetic CdTe layers and holes in the magnetic layers of $\text{Cd}_{1-x}\text{Mn}_x\text{Te}$. The critical magnetic field (B_c) at which the type-I–type-II crossover occurs can be estimated by equating the zero field valence-band offset in Table I and the valence-band edge tuning (E_{VB} , which is 0.8 times the observed energy shift of the magnetic layers as plotted in Fig. 3). A summary of B_c for each of the samples is listed in Table I. It can be seen that the value of B_c increases rapidly with Mn content due to the increasing importance of the antiferromagnetic Mn-Mn exchange. Around this region, in the framework of the ‘‘conventional description’’ of an exciton,¹ a drop in oscillator strength and a plateau in transition energy are expected due to the spatial separation of the carrier wave functions and the rapid change of exciton binding energy.⁵ However, there is no clear signature in the spectra to justify the assignment of a crossover of the band alignment as reported previously.^{1,2} Instead there is a smooth shift in transition energy and a steady decrease in the absorption strength (see Fig. 2). We will discuss this issue later. First, the high field data is analyzed to provide evidence that for sufficiently high fields the transition can be assigned to a type-II band structure.

Above 15 T the magnetic field results for the different manganese contents separate qualitatively into two groups: (a) for $x < 4\%$ the magnetic interaction saturates at low fields, therefore the shift in the optical transition is dominated by the diamagnetic shift (E_{diag}) for both σ_- and σ_+

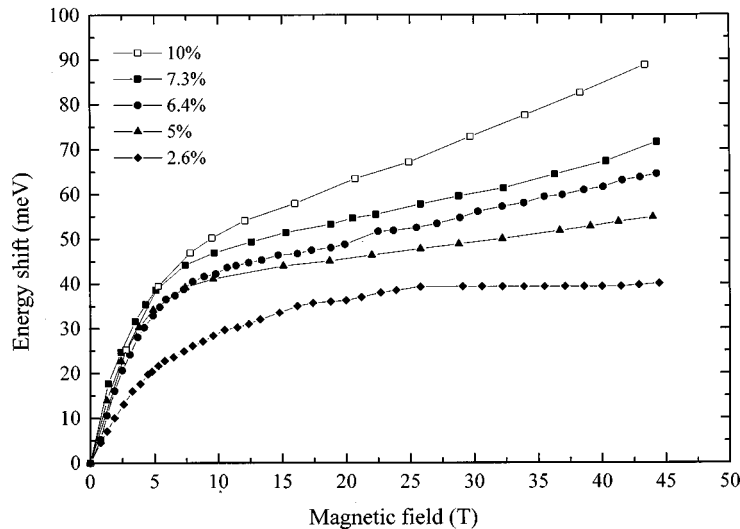


FIG. 3. The observed energy shift of the σ_+ transition of magnetic layers.

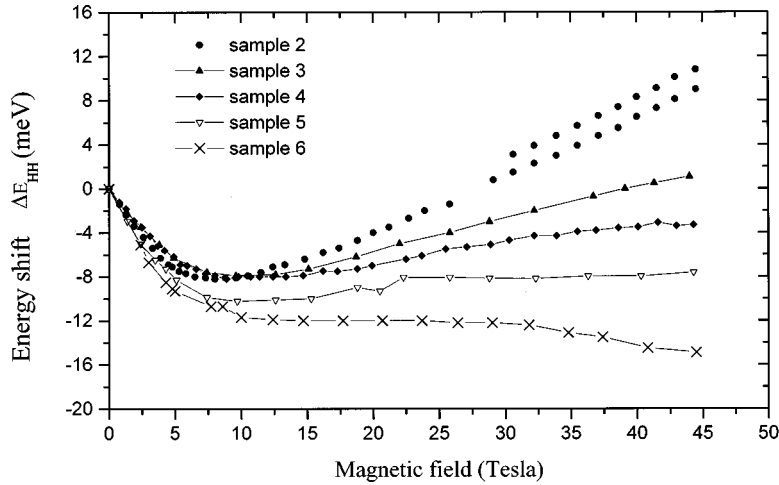


FIG. 4. The energy shift of the σ_+ transition of the quantum wells of the five samples.

transitions (b) for $x > 4\%$ the band-edge tuning in the magnetic layers increases steadily with applied magnetic field up to 45 T. Thus, beyond B_c , the effective band gap of the type-II structure varies directly proportional to the shift of the $\text{Cd}_{1-x}\text{Mn}_x\text{Te}$ band edge. Therefore, in addition to the change of confinement energy and diamagnetic shift, the optical transition energy of the σ_- component also depends on the modulation of effective band gap. The field-dependent transition energy at $B > B_c$ is

$$E(B) = (E_g + E_{\text{vgap}}) + E_e + E_h - E_b + E_{\text{dia}}. \quad (1)$$

In this expression, E_{vgap} denotes the valence-band gap modulation. Its value is equal to the exchange splitting of the valence band in the magnetic layer minus the zero field quantum well potential height listed in Table I. It contributes to the transition energy “only” when the system has swapped over to a type-II band alignment. This quantity is wholly determined by the exchange splitting of the magnetic layers (Fig. 2). For the samples used in this study, the transition energy is dominated by E_{vgap} and E_{diag} due to the slow changes of confinement energy due to the wide width of magnetic layers.

(a) *Low Mn content ($x < 4\%$).* For low concentration samples ($x < 4\%$), there is a qualitative difference in the behavior of the σ_+ and σ_- transitions as shown in Fig. 5 for the sample with $x = 0.026$ (in the diagram only the 1HH exciton and buffer 1s transition are plotted for simplicity). The two transitions split rapidly at low field, followed by a saturation of the magnetic interactions, and above 10 T the diamagnetic shift of the 1s exciton is dominant. As a result the σ_- shows a much smaller increase in energy with field, as the binding energy of the 1s exciton is larger due to the stronger confining potential, and approaches a two-dimensional (2D) character. By contrast the σ_+ transition shows a larger diamagnetic shift than even that of bulk CdTe, indicating that the exciton binding energy is much smaller due to the reduced exciton confinement. As a result the spin splitting actually decreases at high fields. The high field diamagnetic shift of the buffer 1s and both components of the 1HH transition are fitted with the numerical model of Makado using the conduction- and valence-band mass parameters of $m_e = 0.096$ and $m_h = 0.51$.⁹ The result is also shown in Fig. 5 as solid and dashed lines for the bulk CdTe and SL transitions, respectively. The fitting agrees very well with the data and gives the high field excitonic Rydberg

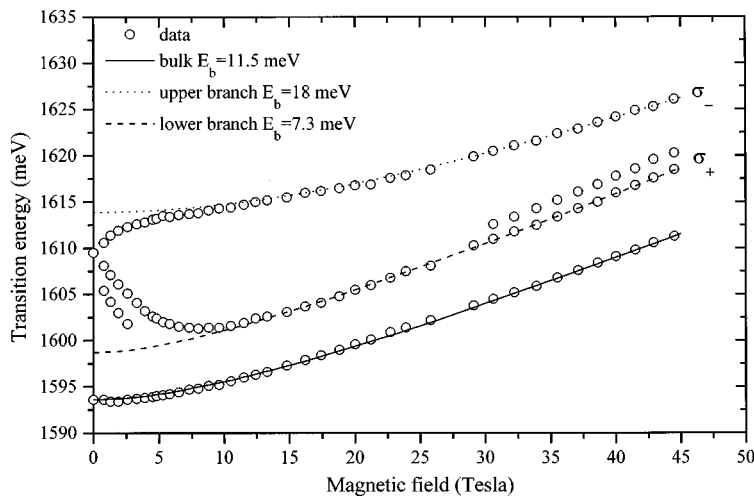


FIG. 5. The fitted high field diamagnetic shift of bulk CdTe (solid line) and 1s HH of SL (dashed and dotted line for σ_+ and σ_- components, respectively) for sample 2.

energies for the σ_- and σ_+ transitions as 18.6 and 7.4 meV, respectively. The value for the σ_+ transition of 7.4 meV is lower than the value for bulk CdTe of 11.5 meV as expected and is therefore consistent with a type-II behavior for the $m_j = -3/2$ spin component for fields above 10 T, with no further change in the confinement potential. A similar behavior is also found for sample 1.

(b) *High Mn content ($x > 4\%$)*. For the samples with high manganese content, the σ_- component of the HH state shows a similar 2D behavior as seen for the low concentration samples. We will not discuss this further. For the σ_+ component, the behavior is different as there is a large contribution to the transition energies from the band-gap modulation [E_{vgap} in Eq. (1)] and is not dominated by the bulklike diamagnetic behavior as for low manganese content. This can be seen in Fig. 4. It shows that the ΔE_{HH} curve moves away from the data of sample 2 as the manganese content increases. For the sample with the highest x value (sample number 6), ΔE_{HH} is nearly unchanged up to 45 T. As the change of confinement energy is very small, this suggests a cancellation of E_{vgap} and E_{dia} .⁵ To provide direct evidence that the σ_+ transition is dominated by the band-gap shift that only occurs for a type-II transition, the energy shift of 1HH is analyzed as a function of the valence-band edge tuning of the magnetic layer (E_{VB}), taking account of the diamagnetic shift of the exciton.

We assume that the high field diamagnetic exciton shift E_{dia} is very similar in samples with a similar structure as has been shown up to 45 T by both experiment and theoretical modeling in the more strongly type-II system of $\text{ZnTe}/\text{Zn}_{1-x}\text{Mn}_x\text{Te}$.⁵ Therefore, to show more clearly the effect of valence-band-edge tuning on the 1HH transition, we subtract the E_{dia} from the data of ΔE_{HH} using the diamagnetic shift calculated and previously fitted to the low Mn content sample 2. These plots are summarized in Fig. 6. At low fields, the energy shift is dominated by the change of confinement energy and binding energy [Eq. (1)]. For high fields, and thus large valence-band-edge shift, there is a clear change in behavior. In this case the shift in 1HH energy is directly equal to the shift in the valence-band-edge tuning, as shown by the line of unity gradient. This is clear proof of the change over to type-II band alignment. It should be noted, however, that it is necessary to achieve a relatively large absolute shift of the valence-band-edge, of order of 50 meV, before it is possible to observe this behavior. The position at which we estimate that the transition to full type-II behavior has occurred is marked by the dashed line for each case in Fig. 6 (the corresponding field is labeled as B'_c). It can be seen that this is at substantially higher fields than B_c , where the type I-type II band-edge crossover occurs. The linear proportionality of $\Delta E_{\text{HH}} - E_{\text{dia}}$ to E_{VB} is only achieved once a type-II offset of at least 15 meV has been achieved. This is consistent with the idea that the type-II valence-band offset has to be larger than the exciton binding energy in order to overcome the Coulomb interaction, leading to the formation of the true type-II exciton. This relatively large type-II band-edge modulation can only be achieved by the combination of a large Mn content and the application of a sufficiently high magnetic field to overcome the antiferromagnetic nearest neighbor exchange.⁶

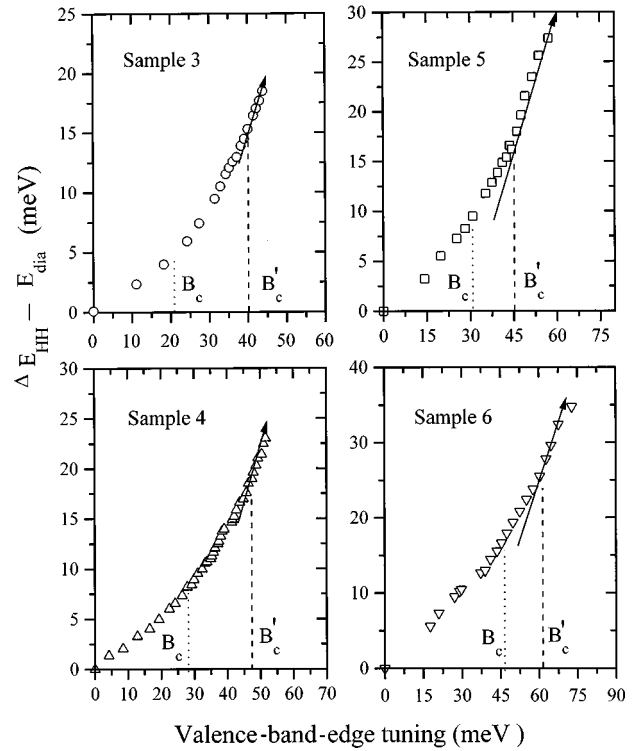


FIG. 6. The change of SL energy of ΔE_{HH} minus E_{dia} verse valence-band-edge tuning.

Below B'_c there is a progressive decrease in the gradient of the line down to B_c , without any single sharp feature. In this region the Coulomb attraction acts in opposition to the quantum confinement effect, which tries to separate the carrier wave functions in different layers, and pulls the electron-hole pair toward the interface. This leads to a progressive redistribution of carrier wave functions, as a result of which the excitonic energy levels modeled by the conventional picture are modified. Quantitatively interpreting the optical transition energy and the oscillator strength requires a self-consistent method to calculate the energy levels in which the Coulomb interaction should be taken into account as demonstrated for the iron-based system by Warnock *et al.*¹⁰ For the sample structures studied here, since the magnetic layers are wide and the barriers relatively small, there is considerable wave-function penetration into the nonmagnetic layer. As a result, the excitonic features in the spectrum are still clear due to the relatively large resulting oscillator strength even for the type-II band alignment.

In summary, magnetorefectivity has been studied in pulsed magnetic fields up to 45 T to probe the type-I–type-II crossover in the $\text{CdTe}/\text{Cd}_{1-x}\text{Mn}_x\text{Te}$ system. The characteristics of the excitonic transition of the σ_+ component of 1HH can be categorized into three regions in which (a) at low field the change of excitonic energy is governed by the change in confinement energy (b) at high fields the valence-band-gap modulation dominates, and (c) there is an intermediate region where Coulomb interaction significantly modulates the band profile preventing the formation of a type-II exciton. By extending the measurements to high magnetic fields, the optical behavior of a field-induced type-II exciton has been demonstrated.

- ¹E. Deleporte, J. M. Berroir, G. Bastard, C. Delalande, J. M. Hong, and L. L. Chang, *Phys. Rev. B* **42**, 5891 (1990).
- ²E. L. Ivchenko, A. V. Kavokin, V. P. Kochereshko, G. R. Posina, I. N. Uraltsev, D. R. Yakovlev, R. N. Bicknell–Tassius, A. Wang, and G. Landwehr, *Phys. Rev. B* **46**, 773 (1992).
- ³S. Kuroda, K. Kojima, K. Kobayashi, K. Uchida, N. Miura, and K. Takita, in *Proceedings of the 11th International Conference of High Magnetic Field in Semiconductor Physics*, edited by D. Heiman (World Scientific, Singapore, 1995), p. 662.
- ⁴B. Kuhn–Heinrich, W. Ossau, H. Heinke, F. Fisher, T. Litz, A. Waag, and G. Landwehr, *J. Appl. Phys.* **63**, 2932 (1994).
- ⁵H. H. Cheng, R. J. Nicholas, M. J. Lawless, D. E. Ashenford, and B. Lunn, *Phys. Rev. B* **52**, 5269 (1995).
- ⁶R. J. Nicholas, M. J. Lawless, H. H. Cheng, D. E. Ashenford, and B. Lunn, *Semicond. Sci. Technol.* **10**, 791 (1995).
- ⁷E. D. Isaacs, D. Heiman, X. Wang, P. Becla, K. Nakao, S. Takeyama, and N. Miura, *Phys. Rev. B* **43**, 3351 (1991).
- ⁸J. A. Gaj, R. Planel, and G. Fishman, *Solid State Commun.* **29**, 435 (1979).
- ⁹P. C. Makado, *J. Physica B* **132**, 7 (1985); P. C. Makado and N. C. McGill, *J. Phys. C* **19**, 873 (1986).
- ¹⁰J. Warnock, B. T. Jonker, A. Petrou, W. C. Chou, and X. Liu, *Phys. Rev. B* **48**, 17 321 (1993).